Fermilab Tevatron Quadrupoles

TM-1183
1620.000
March 1983

W. E. Cooper, H. E. Fisk, D. A. Gross†, R. A. Lundy, E. E. Schmidt & F. Turkot
Fermi National Accelerator Laboratory*
Batavia, Illinois 60510

Abstract

Details on the design, construction, and performance tests of Energy Saver/Doubler quadrupoles are presented along with recent data from the test of a special high gradient low beta prototype quadrupole.

I. Introduction

The Fermilab Tevatron superconducting accelerator will use both dipoles and quadrupoles as the main magnetic elements to accelerate and store its proton and antiproton beams. The machine design calls for 774 4.4T dipoles and 216 quadrupoles with maximum gradient of 19.3 kG/in.[1] We have designed and fabricated two shell quadrupoles using standard Fermilab wire and collaring techniques. In addition to the 2 3/4" aperture 66.1" long standard quadrupoles we have also built special quadrupoles to satisfy Tevatron lattice requirements that vary in length from 25 to 99 inches. Details on the design, construction, and test performance of these quadrupoles are presented here along with results from tests of a special (25.5 kG/in.) high gradient prototype low beta quadrupole.

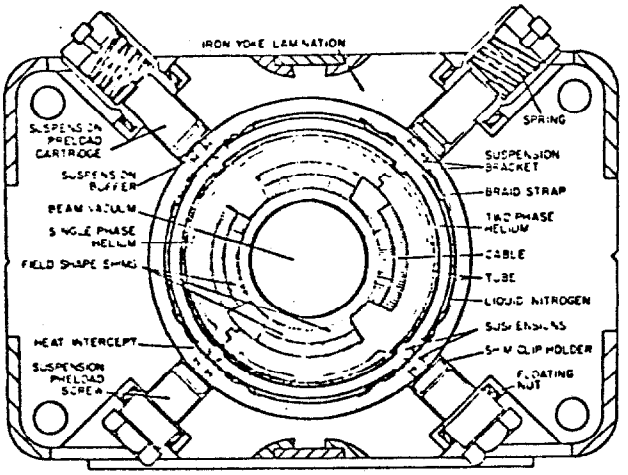

Fig. 1 Tevatron quadrupole cross section.

II. Design

The cross section of the warm iron, cold bore Tevatron quadrupole is shown in Figure 1 and the specifications and dimensions are given in Table 1. Conceptually the design is similar to the Fermilab dipole that relies on two circular shaped superconductor shells where the unwanted normal 6 and 10 pole moments can be cancelled by adjusting the azimuthal angles at which the inner and outer shells terminate. In the quadrupole case that cancelling geometry is not similarly possible. Further constraints on the quadrupole require the gradient to track the dipole's central field with the same current and the clear central aperture must also be similar. In fact, the quadrupole inner shell radius was chosen to be slightly larger than the dipole bore to allow placement of multipole correction coils inside the quadrupoles. These and other considerations led to a design with the inner shell of conductors divided into two blocks separated by a stainless steel spacer. The high field point, which determines the minimum requirements for the superconductor short sample limit, is located on the inner shell block of six cables nearest the pole. At the maximum design gradient of 19.3 kG/in (4440 A) the field on that conductor is 4.1 T.

Table 1
Quadrupole Coil/Cryostat Parameters & Specifications

	Inner Coil	Outer Coil	
Inner Radius	1.750	2.088	in.
Outer Radius	2.067	2.405	in.
Key Angle	30.1194	30.7839	deg.
No. Turns	14	20	
Conductor Required	210 (x4)	280 (x4)	ft.

Assembly Dimensions (all in in.):	
Inner Collar Radius:	2.433
Outer Collar Radius:	2.933
Ground Wrap Material/Thickness:	Kapton/0.028
Coil Length (Actual):	69
Coil Length (Magnetic):	66.1
Yoke Length:	63
Yoke Inner Radius:	4.000
Yoke Outside Dimension:	9.750x15.478
Overall Slot Length:	163

	Inside Rad. (In.)	Material Thickness (In.)
Beam Tube	1.372	0.065
1 Phase Tube	3.040	0.036 (20 GA)
2 Phase Tube	3.177	0.036 (20 GA)
Inner Shield Tube	3.389	0.049 (18 GA)
Outer Shield Tube	3.552	0.036 (20 GA)
Vacuum Tube	3.963	0.036 (20GA)

The net forces at full field on each cable are shown in Figure 2. Mechanical motion of the conductors is arrested with stainless steel collars similar to those used in the dipoles. In the collaring process azimuthal preload that exceeds the maximum Lorentz force is applied to keep the conductors from moving when energized with current. The odd harmonic multipoles of the quadrupole, namely 12 and 20 pole, can be adjusted to acceptably small levels (.0001 of the quadrupole field at a radius of one inch) by slightly shifting the relative azimuthal positions of the 6 and 8 conductor blocks.

The cryostat and outer iron are again very similar to those used in the Fermilab Tevatron dipole.[2] The cross section of the cryostat shown in Figure 1 illustrates the vacuum regions on either side of the nitrogen shield and the paths for both single (liquid) and two phase (liquid plus gaseous) helium. To avoid heat leaks the concentric regions of the cryostat are suspended from one another by small fiberglass and epoxy (G-10) standoffs. The collared coil azimuthal location within the cryostat is kept stable during thermal cyclying with welded

* Operated by Universities Research Assn. Inc., under contract with the U.S. Department of Energy.

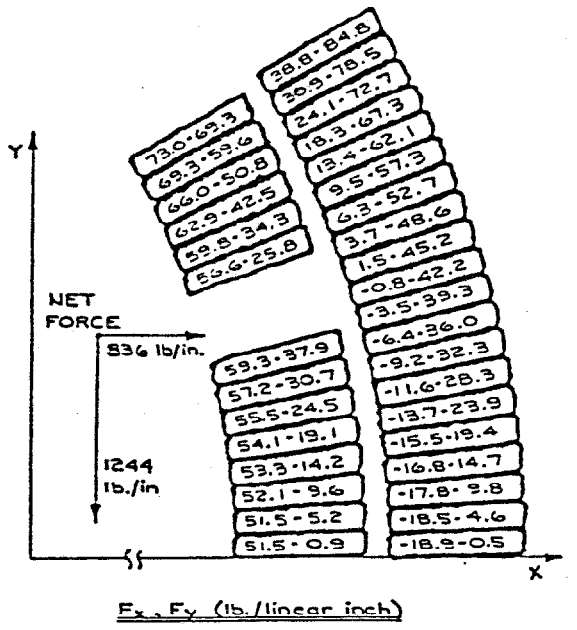

Fig. 2 Force diagram for one octant of a Tevatron quadrupole.

tabs between the collared coil and inner cryostat. The location of the outside of the cryostat is stabilized with bolts as shown in Figure 1. The bottom and top bolts contact the cryostat at 28 in. intervals where the G-10 standoffs are located. The top bolts are spring loaded so that during cooling, when the collared coil shrinks approximately 25 mils diametrically, the bolts continuously contact the cryostat and keep it stably oriented.

Outside the cryostat there is a laminated iron yoke that provides a flux return path for the quadrupole field. Image current in the iron accounts for 7.08% of the total magnetic field. The iron also provides a rigid mechanical structure which is needed for stability and safety.

III. Construction

The Rutherford style superconducting cable used in the magnets is made from 23 strands of 0.0268 in. diameter NbTi in copper with a Cu to SC ratio of 1.8 to 1. The cable is keystone in cross section (0.055" x 0.307" x 0.044") and is wrapped with 0.002 in. thick kapton insulation and 0.007 in. thick epoxy impregnated fiberglass tape. Each strand of the cable contains about 2000 SC filaments (8μ diameter) and alternate strands of the cable are coated with Staybrite solder or Ebonal (CuO) for proper current sharing among the strands. Short sample data on the wire are given in a paper by W. Fowler et al.[3]

Four separate coils are made for each quadrupole. The inner shell of each coil is wound on a mandrel and heat cured in a press. This causes the epoxy impregnated in the fiber glass to flow and form a bond thus making the coil rigid and dimensionally correct. The outer conductor shell is similarly wound on the inner, with an appropriate spacer between them, and a second heat cure provides a single coil. One of the four coils has a through cable called the buss to allow the series connection of magnets. This buss is specially insulated with a double wrap of kapton (4mils) to standoff the high voltage which could develop during quenches. Each coil's azimuthal size is measured under azimuthal load to determine both coil size and bulk modulus. These data are used to match individual coils that make up a magnet. Typically the coil sizes vary about 5 mils and the general rule is to match coils of similar size. Simple resistance and inductance measurements are performed on each coil to guarantee its integrity.

The four selected coils are mounted on an assembly mandrel and 5 pre-formed layers of 5 mil kapton (ground wrap) are used to insulate the coils from the coil armor and collars. Initially this ground wrap had holes in it to help communicate liquid helium from the outside of the bore tube to the coils, but during hi-pot tests with gaseous helium the holes in the kapton allowed glow discharge at about 900V. Thus the holes were eliminated. At the ends of the coils, in the region of the G-10 saddles, special collars and ground wrap are used. Care is taken to overlap the various layers of ground wrap such that at least 0.5 inches of path length is encountered by any potential electrical discharge. It should be noted that no heaters are installed in the quadrupoles since the stored energy of 70 kJ at 4500A is small enough to pose no serious problem during quenches. With the insulation in place the collars are stacked loosely on the vertically hanging coils plus mandrel prior to their insertion in the press. The collaring press is a hydraulic device that simultaneously applies force on four sides of the magnet and thus closes the collars permitting the insertion of keys to lock the collars. The press typically exerts a radial pressure of 15,000 lbs. per linear inch in closing the collars.

The mandrel is then pulled from the collared coil and electrical checks are again performed on each of the four separate coils. At the downstream end of the quadrupole the leads from the individual coils are soldered together using special heat sink blocks so as not to damage the kapton insulation which has been unwrapped to allow the soldering. Hi-pot tests in atmospheric gaseous helium showed these buss work regions to be inadequately insulated for voltages which might be as high as 1500V. To cure this problem three layers of 2 mil kapton are wrapped around each exposed coil splice and special kapton sleeving is placed around the buss as it exits the coil package. In addition a top-hat piece of G-10 is used to cover the buss work and to insulate it from the stainless steel beam pipe and end cap which covers the buss work. Again the rule of thumb is to provide at least 0.5 inches of path length for potential sparks.

At this stage the collared coil has its integral gradient and magnetic multipoles measured at room temperature using a low power AC technique.[4] Results from these measurements can be used for feedback in the manufacturing process and also provide a base of data for later comparison with cold measurements.

The collared coil is then inserted into a pre-manufactured cryostat. At this stage the beam tube with its attached beam detector is welded in place.[5] After plumbing work is completed the cryostat is checked for leaks and the iron yoke is installed around it.

IV. Test Procedures and Results

Each magnet undergoes an extensive set of tests under full operating conditions to verify its suitability for accelerator use.[6] A magnet is mounted on a test stand, precision leveled, connected to cryogenic end boxes and leak checked. Cool down to 4.7°K takes three hours. A warm bore tube of 1.95 in. inside diameter allows access to the field region. The following series of tests, taking about 10 hours, are then performed on the magnet.

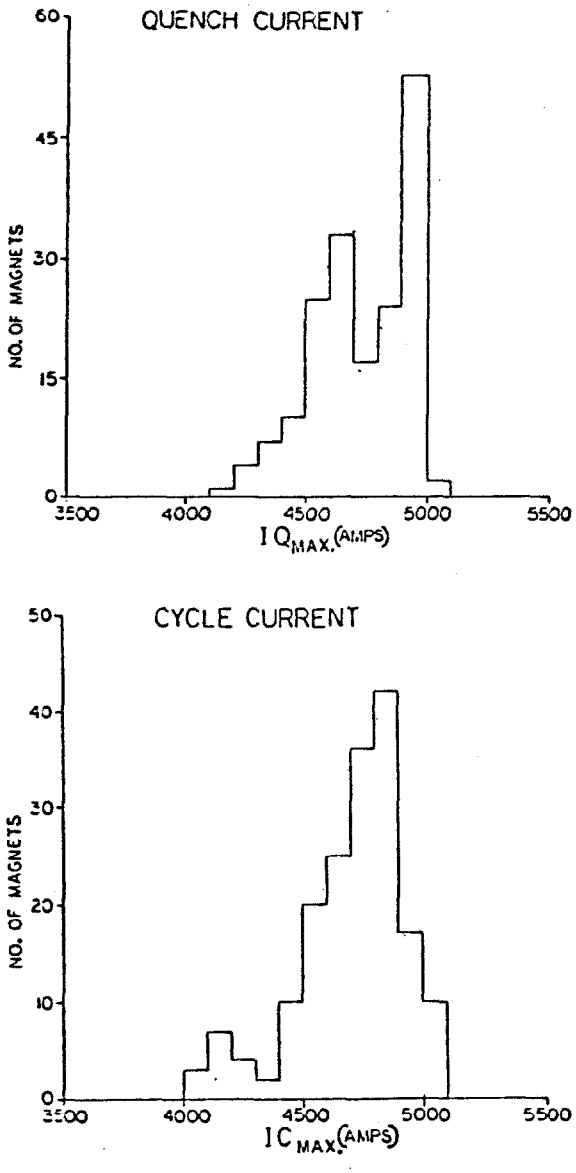

Fig. 3 Quench and Cycle current histograms. Fig. 3a is the quench current histogram and Fig. 3b is the cycle current histogram.

A. Maximum Current Capability

With the warm bore filled with LN_2 a linearly rising current ramp is applied until a quench occurs. The slope for the initial ramp is 700A/sec, and 230A/sec for all subsequent ramps. The test is terminated if the current reaches 5000A (power supply limit) or when the maximum current (IQmax) achieved on two successive ramps differs by 50A or less. The IQmax distribution for 138 quads is given in Figure 3a. The mean value is 4780A and the r.m.s. width is 170A. About 1/3 of the magnets reach 5000A and the average number of quenches is 2.6. A second test uses a cyclical accelerator-ramp current waveform that has a linear rise of 200A/sec, a 20 sec long flat top, and a linear fall. The flat top current is incremented 50A every two cycles until a quench occurs on or near flat top. The distribution of maximum current, ICmax, for the test is shown in Figure 3b. The average ICmax is 4770A with an r.m.s. of 160A. The cryogenic conditions for these

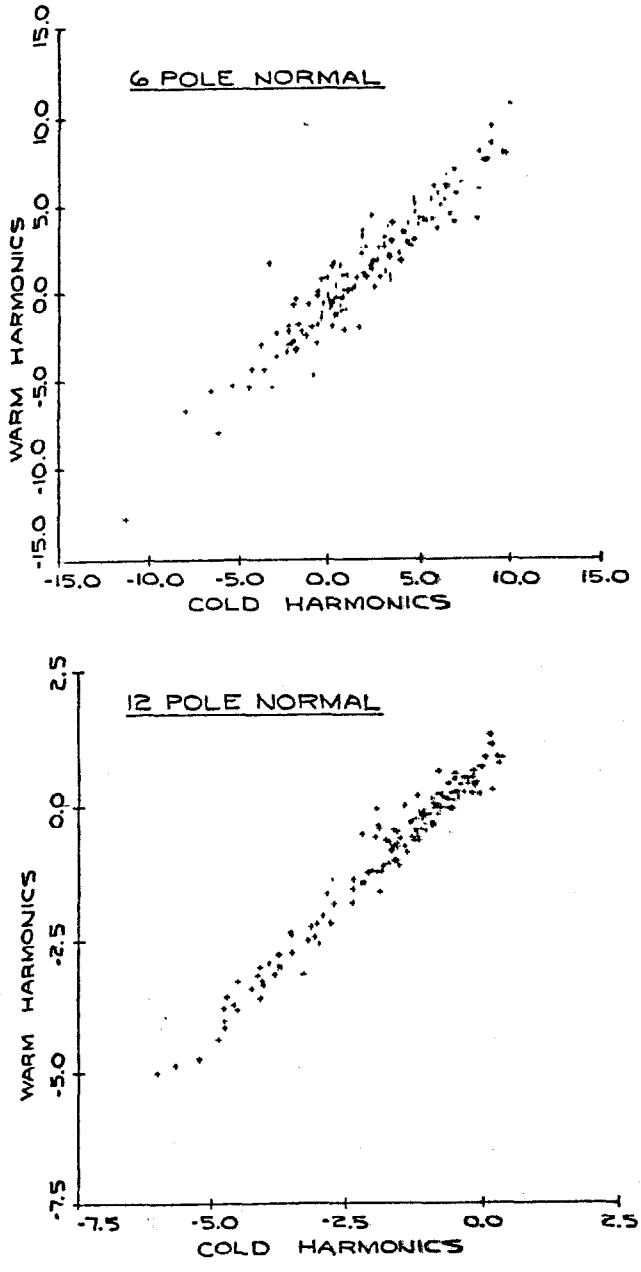

Fig. 4 Warm and cold harmonic correlations. Figs. 4a and 4b are the normal 6 and 12 pole harmonic correlations, respectively.

tests are as follows: one-phase liquid He at both ends of the magnet in the range 4.65 - 4.70°K, subcooling of 1 psi or better, and a mass flow of ~24 g/sec.

B. Field Harmonics vs. Current

As mentioned in Section III, harmonics are measured at low power and room-temperature on the bare collared coils using an 84 in. long Morgan coil of radius 1.1 in.[6] For the cold tests a rotating coil probe of length 94 in. is employed[7]; the coil samples the field out to a radius of 0.92 in. from the quad center. Measurements are preceded by two standard ramp cycles to 4000A. Harmonics are measured at 7 standard currents between 200A and 4000A in a single run. Two measurements are done at each current with one being taken on the way up and the other on the way down. Care is exercised to ensure that the current goes from one set point to the next in a monotonic fashion. Overshoots are kept below 0.2A. The integrated induced signal from the coil rotation is Fourier analyzed up to a term $\cos(15\theta + \alpha)$. The harmonic coefficients obtained are then transformed to a coordinate system in which the dipole coefficients are zero.

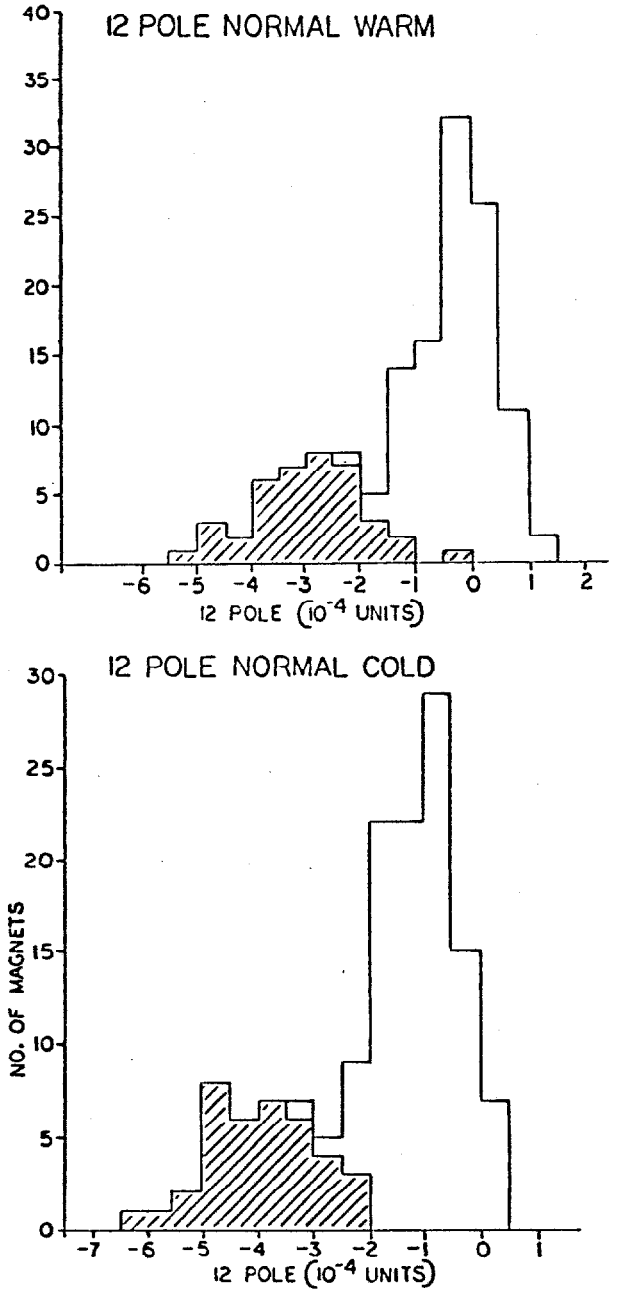

Fig. 5 Warm and cold normal 12 pole moments. The cross hatched data represent quadrupoles manufactured before a shim change was made to reduce the magnitude of the normal 12 pole.

The correlation between harmonics measured at room temperature (I=10A) and at 4.7°K (I=4000A) is generally quite good. Figure 4 exhibits the correlation for the normal sextupole (b_2) and the normal 12-pole (b_5) for a sample of 143 magnets. A unit on this figure is 0.0001 times the quadrupole field at a radius of one inch. The normal 12-pole distributions measured warm and cold are given in Figure 5. The shapes are similar, but the warm distribution is clearly shifted toward more positive values by one unit. The two-peak distribution is a result of a design change made in the geometry of the superconducting coil to reduce the magnitude of the 12-pole. In Table 2 we list for both warm and cold measurements the mean values and r.m.s. widths of the distributions for all harmonic coefficients whose mean values are greater than 0.1 in magnitude. In addition to the shift between warm and cold mentioned above for the 12-pole, there is also a shift in the sextupole for both normal and skew coefficients. These shifts can be partially understood in terms of a small systematic offset observed between the center of the quadrupole field and the center of the magnet yoke.

Table 2
Quadrupole Harmonic Coefficients

	Normal				Skew			
Pole	Cold		Warm		Cold		Warm	
	Mean	σ	Mean	σ	Mean	σ	Mean	σ
6	2.09	3.75	1.39	3.69	2.97	3.36	1.05	3.43
8	1.28	0.90	1.22	0.88	-0.33	2.01	-0.60	1.95
10	-0.31	0.69	-0.34	0.63	-0.62	0.75	-0.68	0.71
12	-1.81	1.47	-0.99	1.46	0.23	0.37	0.16	0.26
14	0.04	0.27			0.17	0.27		
18	-0.06	0.24			-0.11	0.22		
20	-1.68	0.29	-1.76	0.25	0.22	0.29	0.01	0.12
24	-0.11	0.22			-0.07	0.23		
28	0.76	0.29			-0.16	0.25		

Since the small magnitude of the 12-pole results from a cancellation between the various conductor blocks of the coil, a current hysteresis is expected in b_5. The dashed curve in Figure 8 shows the effect for a standard 66 in. quadrupole. The hysteresis effect gives rise to Δb_5 of 3.8 units at injection energy for the Saver.

C. Integrated Field Gradient

A precision quadrupole Morgan Coil made from four, 0.004 in. tungsten wires stretched through the warm bore (coil radius 0.795 in.) is used to measure $\int G dl$ as a funtion of magnet current. The distribution at 4000A for a sample of 151 magnets is given in Figure 6. The mean value at a radius of one inch is 1151 KGm/m and the width is ±0.20%. The distribution has been widened somewhat due to an

intentional change in coil size. The curve in Figure 6 is a fit to the first 114 magnets produced. Its width is ±0.14%. As a function of current the transfer constant increases by 0.3% between 660A and 4400A.

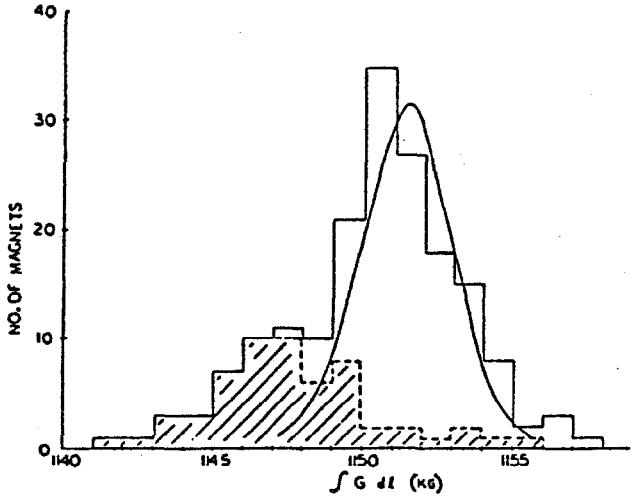

Fig. 6 Integral of the gradient. The cross hatched data are for quadrupoles manufactured after a change in the dimensions of the winding mandrels. The curve represents a fit to data from magnets produced before the coil size was changed.

D. A.C. Loss

A. C. loss measurements were performed on the first 40 magnets using integration technique of Wake et al.[8] In an accelerator ramp cycle between 400A and 4000A at a ramp rate of 200A/sec, the energy deposition in the magnet is 120J. Variation of the ramp rate from 50A/sec to 300A/sec, increases the A.C. loss by 12%.

E. Voltage Standoff Capability

D. C. hipot tests from coil to ground are made on each magnet with pure He in the coil region. The test conditions are as follows:

	Pressure	Temp.	Vmax	Vmin
a)	15 PSIA	295°K	1.0 KV	0.8 KV
b)	60 PSIA	295°K	2.1 KV	1.9 KV
c)	22 PSIA	4.7°K	2.4 KV	2.1 KV

Acceptable magnets must exceed Vmin in all three tests with leakage currents below 2μa. Two magnets out of 150 have failed to pass these criteria.

F. Field Orientation

The field direction is measured with a pair of stretched wire loops and is subsequently encoded on survey lugs attached to the vertical sides of the magnet's yoke. This is done with a precision of ±0.25 mrad. The field direction is required to be perpendicular to the top of the magnet yoke within a tolerance of ±7.5 mrad. The average center of the quadrupole is measured with the same probe. This information is also transferred to survey lugs mounted on the magnet yoke with a precision of ±0.005 in. Averaged over 80 magnets, the field center is 0.004 in. low with respect to the center of the iron yoke and horizontally it is centered. The standard deviations are 0.009 in. and 0.006 in. respectively.

G. Field Direction With Thermal Cycling

Five magnets were each subjected to a series of 14 thermal cycles (275°K to 4.7°K) to evaluate the stability of the field direction under such conditions. A plot of the field direction vs. thermal cycle number is seen in Figure 7 for one of the five magnets. No simple trend is evident. The average of the standard deviations for the five magnets is 0.24 mrad. There is a suggestion that the difference between the first and second cycle may be larger than subsequent cycles. Any secular trend appears to be less than 0.03 mrad per cycle with no preferred direction of change.

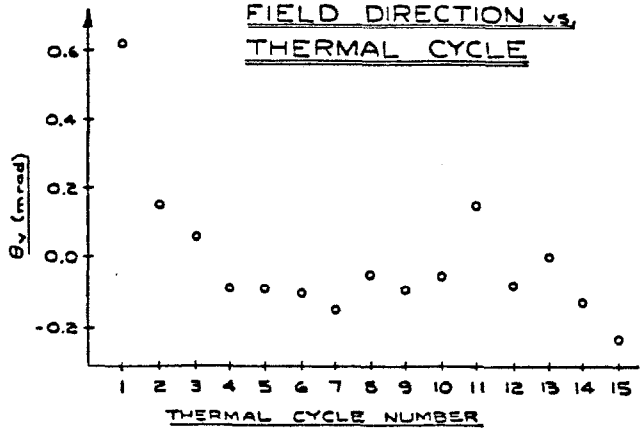

Fig. 7 Field direction vs thermal cycle number.

V. Low Beta Quadrupoles

Measurements have been made on a 66 in. quadrupole magnet which was built with a superconductor cable developed for use in low beta quadrupoles. The cable differs from the standard Fermilab cable in that the filament diameter is 20 microns instead of 8 microns, the copper/superconductor ratio is 1.3 instead of the standard cable ratio of 1.8, and all 23 strands of the cable are coated with Staybrite. Measurements made on the cable indicate that it will reach 452°K (the melting point of solder) at 4.9 ±0.4 Miits.[9] Unlike standard Fermilab quadrupoles, this magnet was built with heaters similar to those used in dipoles to aid in quench protection. In other respects, the magnet was the same as standaard 66 in. Fermilab quadrupoles.

The quench current was measured to be 6078A at 4.68°K and 6331A at 4.60°K with a ramp rate of 373 A/sec. The short sample limit for the quadrupole load line is extrapolated to be 6290A (5.79T) at 4.60°K from short sample tests done in 6.50T and 7.07T fields at 4.29°K[10]. Heater induced quenches were run with the dump resistor shorted in which case

the magnet absorbs all of the energy except for that dissipated in the 15 milliohms of busswork. At a quench current of 4780A the magnet absorbed 4.3 Mjits. This suggests that special provisions will be needed in the ring to provide quench protection for these magnets. The AC loss per ramp cycle was measured to be 260 joules ramping to 6000A. This is higher than the loss extrapolated for quadrupoles with standard cable (185 joules per ramp cycle) as would be expected from the difference in cable.

Results of measurements of the integrated field gradient agree with those of standard quadrupoles and show no iron saturation up to the highest current at which the measurements were done: 5400A. At this current, the ratio of integrated field gradient to current was still increasing by 0.042% per 1000A. Extrapolation of the measurements to 6331A gives a field gradient of 27.6 kG/in. at this current. Harmonic coefficients were measured up to a current of 6013A. The results are not unusual except for the normal 12-pole coefficient which shows a larger hysteresis than in quadrupoles made with the standard conductor as can be seen in Figure 8. This reflects the change in persistent currents from the different filament size of the conductor. No evidence of conductor motion is seen in the harmonics.

The design of full scale low beta quadrupoles is proceeding based on these favorable results.

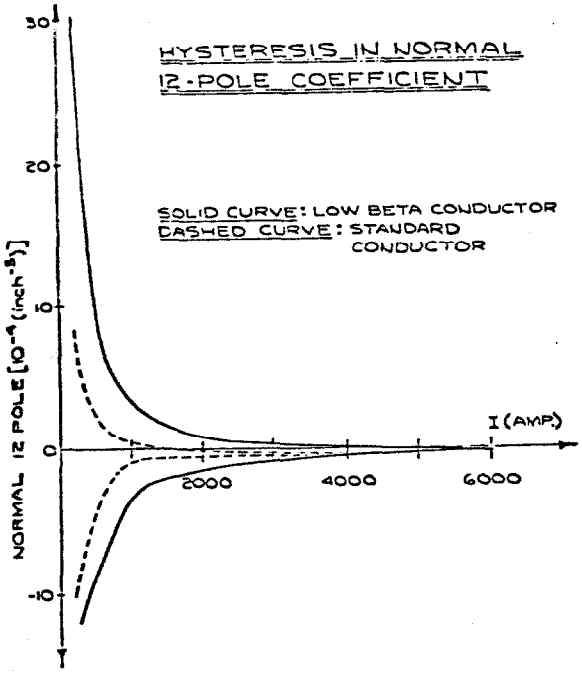

Fig. 8 Current hysteresis in the normal 12 pole moments versus current. The dashed curve is the average data from several Tevatron quadrupoles and the solid curve derives from measurements of the low beta prototype quadrupole.

Acknowledgements

Many people have contributed to the quadrupole effort and in particular we want to acknowledge the substantial contributions of our colleques: B. Brown, J. Carson, D. Edwards, N. Engler, R. Hafnt, M. Johnson, G. Kalbfleisch, K. Koepke, P. Mantsch T. Nicol, J. O'Meara, H. Pfeffer, R. Rajendran, S. Snowdon, and A. Tollestrup.

† Present address: General Electric Research Center, Schenectady, New York.

References

1. A Report on the Design of the Fermilab Superconducting Accelerator May, 1979 (unpublished), Fermilab.
2. G. Biallas et al., IEEE Trans. Magn. MAG-15 131(1979). There is also a technical memo titled "A Design for Cryostat Supports for the Fermilab Energy Saver/Doubler" by J. E. O'Meara, G. Biallas, J. Carson, T. N. Lincicome, R. A. Lundy, F. Markley and R. J. Powers available from the authors P. O. Box 500, Batavia, Illinois 60510.
3. Fowler, W. et al, IEEE Trans. on Mangetics MAG-17, 925 (1981)
4. H. E. Fisk et al., IEEE Trans. on Magnetics MAG-17, 420 (1981)
5. R. Shafer, R. Webber and T. Nicol. IEEE Trans. on Nucl. Sci. NS-28 Vol 3, 2290 (1981)
6. D. A. Gross et al., IEEE Trans. on Magnetics, MAG-15,137 (1979)
7. M. Wake et al., Cryogenics, 341 (1981)
8. M. Wake et al., IEEE Trans. on Magnetics, MAG-15, 141 (1979)
9. The standard Fermilab wire is rated at 7 Mjits; see K. Koepke et al; IEEE Trans. on Magnetics MAG-17,713 (1981).
10. A. Mc Inturff, private communication